The Seeding Effects on the Phase Transformation of Sol-Gel Derived PZT Powder

Hyun Tae Lee, Wan In Lee,[†] Yoo Hang Kim,[†] and Chin Myung Whang[*]

School of Materials Science and Engineering and Institute of the Advanced Materials
[†]Department of Chemistry and Center for Chemical Dynamics, Inha University, Incheon 402-751, Korea
Received April 1, 2002

The formation temperature for the perovskite lead zirconate titanate [Pb(Zr,Ti)O$_3$, PZT] derived from sol-gel route was lowered by more than 100 $^{\circ}$C with the addition of crystallographically suitable seed particles, such as barium titanate (BT) or PZT. We investigated the effect of seeding on the crystallization of perovskite phase and on the microstructure of the sol-gel derived PZT powder by varying the concentration, size and chemical species of seed particles. The phase transition as a function of temperature was monitored by DTA, XRD, and Raman spectroscopy, and the interface between the seed particle and grown PZT layer was analyzed by SEM and high resolution TEM techniques. It was found that both the heterogeneous and homogeneous nucleation contributes competitively in the formation of perovskite PZT grains.

Key words : Seeding effect, PZT Powder, Sol-gel, Microstructure, Raman

Introduction

The lead zirconate titanate [Pb(Zr,Ti)O$_3$, PZT] system has been studied since 1950s.[1] The perovskite PZT demonstrates high dielectric constant and large ferroelectric, piezoelectric, pyroelectric and electro-optics responses when subjected to an applied electric field. Many applications[2] such as transducers, ferroelectric memories, sonars, optical filters, shutters, actuators and modulators are under development.

Considerable works have been reported on the sol-gel preparation of PZT materials.[3-6] They are mainly concerned with precursor chemistry, structural evolution *via* sol-gel transition, crystallization behavior of the derived xerogels during thermal treatment, and the electrical properties related to the chemical and processing conditions. During the synthesis of several lead-based perovskites, including PbTiO$_3$ (PT), PZT and (Pb, Mg)NbO$_3$ (PMN), the formation of a non-ferroelectric pyrochlore phase (cubic Pb-deficient) is commonly observed and the amount of unwanted pyrochlore phase varies depending upon processing conditions.

It has been shown[7-10] that the addition of crystallographically suitable seed particles modifies the phase selection, lowers the crystallization temperature from an amorphous precursors or modifies the microstructural development during polymorphic transformation. Thus, seeding provides a new method for ceramic process that has been largely unexplored. To minimize or eliminate the formation of pyrochlore phase, perovskite seeding technique has been employed to control the crystallization in sol-gel derived lead-based perovskite powders and films.[11-16] For example, perovskite seeding has been reported to decrease the perovskite formation temperature of PMN from the metastable pyrochlore intermediate by almost 75 $^{\circ}$C,[11] which implicates that

PMN formation can be controlled by perovskite seed additions. Carvalho and coworkers[12] studied PMN crystallization behavior from BaTiO$_3$ (BT) seeded and BT-doped PMN-carboxylate gels. The addition of BT increased the perovskite fraction from 88% to 95% after heating at 800 $^{\circ}$C for 1 hr. Messing *et al*.[8] found that the addition of BT seed particles to a PMN-EDTA precursor reduced not only the perovskite crystallization temperature from 700 $^{\circ}$C to 600 $^{\circ}$C, but also the nonferroelectric pyrochlore phase from 14% to 2%.

In the case of PZT powder, Nass *et al*.[14] demonstrated that the formation temperature of pure perovskite phase was lowered by 50 $^{\circ}$C through the introduction of 5 wt% PZT seeds. Also, Othman and Hayashi[16] reported that perovskite formation temperature of the PZT film could be effectively lowered to 450 $^{\circ}$C with multi-seeding layers. Chen and Mackenzie[17] studied the formation kinetics of the perovskite phase of sol-gel derived PZT films, and showed that the perovskite transformation was nucleation-controlled.

They described the transformation kinetics as:

$$A \xrightarrow{k_1} Py \xrightarrow{k_2} Pe$$
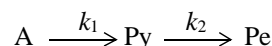
in which A, Py and Pe represent amorphous, pyrochlore and perovskite phase, respectively. The activation energy calculated for perovskite formation was 26 kJ/mol. Since nucleation is the rate-determining step of the phase transformation, its kinetics can be accelerated when numerous nucleation sites are created in the matrix. Therefore, we tried to prepare pure perovskite PZT powder at a low temperature using the concept of controlled seeds, such as BT and PZT seeds. The purpose of this work is the intimate investigation for the effect of the concentration, size and type of the seed on the crystallization temperature of the perovskite phase, yield of perovskite phase, and the microstructure of the sol-gel derived PZT powder.

---

[*]Corresponding author. Fax: +82-32-874-3382, E-mail: cmwhang
@inha.ac.kr

Experimental Section

Lead-zirconate-titanate was synthesized using a morphotropic phase boundary composition with a Zr/Ti molar ratio of 52/48, which is known to exhibit the highest dielectric and piezoelectric properties in the bulk. The precursor materials used were lead acetate trihydrate $Pb(CH_3COO)\cdot 3H_2O$ (Fluka > 99.5 wt%), titanium isopropoxide $Ti(O^iPr)_4$ (Aldrich, 97%) and zirconium propoxide, $Zr(OPr)_4$ (Aldrich, 70 wt% in 1-propanol). Ti and Zr precursors were separately dissolved in 2-methoxyethanol. The solution was heated at 110 °C to reflux for 4 hours. The lead acetate powder was dissolved in 2-methoxyethanol and then refluxed at 120 °C for 4 hours prior to removal of water by distillation. Then, a reaction was performed between Pb solution and Ti and Zr solutions by heating the mixture at 120 °C under reflux for 8 hours. Extra lead acetate trihydrate (5 mol%) was added to the solution to compensate the loss of lead during the thermal treatment. For the complete hydrolysis excess water (Rw, mole ratio of H_2O/PZT = 30) was added to the solution. The resulting sol solution was allowed to gel in an oven at 100 °C for 3 days, yielding brown powders which were then calcined at various temperature ranging from 400 °C to 700 °C for further characterization.

The PZT powder calcined at 700 °C for 1 hour was milled with an attributor using ZrO_2 balls in alcoholic medium. The ground powders with different particle sizes were characterized as single perovskite phase by XRD technique and were used as PZT seeds. The $BaTiO_3$(BT) seeds were commercially obtained from Soekawa Chemical, Japan. The various size of BT (average particle size: 1.2 and 0.2 μm) and PZT (average particle size: 1.2 and 0.2 μm) were separated by a centrifugal sedimentation method. These powders were used as seeds, by dispersing them in 2-methoxyethanol in an ultrasonifier.

The PZT or BT seed with different content was added to the complex alkoxide solution (PZT sol solution) and uniformly dispersed prior to gelation. Following gelation, the seeded PZT gels were dried at 100 °C and then calcined at various temperature.

Thermal behavior of the seeded and unseeded gel powders was analyzed by Differential Thermal Aanalysis (DTA)-Thermogravimetric Analysis (TGA) (Model SDT 1500, TA Instrument) in air at a heating rate of 10 °C/min. A Philips X-ray powder diffractometer (Model PW-170) using Cu-K$_\alpha$ radiation at 40 kV was employed after each heat-treatment to identify the crystal polymorphs, and the relative peak intensity was used to estimate the proportion of each polymorph.

Microstructure of each sample was determined by scanning electronic microscope (SEM, Hitachi, X-650) and the crystallization process was examined by transmission electron microscope (TEM, Hitachi, 9000MA). Raman spectra of the seeded PZT powders were recorded using a Spex Raman spectrophotometer. The Argon ion laser beam with a 514.5 nm line was used as an exciting source. Output of the incident laser power was about 500 mW. Resolution of the spectra was 5 cm^{-1}.

Results and Discussion

Differential thermal analysis of the unseeded PZT gel powder treated in an oven at 100 °C, shown in Figure 1, exhibited a strong exothermic peak between 200 °C and 300 °C corresponding to the large weight loss observed by TGA. This peak was attributed to the decomposition of most of the bound organic species. The weight loss proceeded even after 300 °C, yielding a constant value near 600 °C.

It has been demonstrated by Payne *et al.*[18] that the exothermic feature at higher temperature region varies with process conditions. They discussed the position of the higher exothermic peak observed at ~500-600 °C which varied with water content. According to their report, all reactions were completed by 600 °C in low-water gels (Rw = 2.0 and 3.0), whereas high-water gels (Rw = 10) displayed more diffuse behavior with several peaks and required temperatures up to ~800 °C to complete the reaction. They correlated this behavior with the formation and development of the perovskite phase. However, in our study, a very weak single peak was found at around 500 °C in the higher temperature region for unseeded PZT gel powder which had been prepared with very high Rw value (Rw = 30). Apparently, the processing conditions other than the Rw value exerted greater influence upon the thermal behavior of the sample.

In Figure 2, the DTA curves of PZT gel powder, without and with seeds such as PZT and BT, are shown. The DTA peak in seeded gels was narrower than that in unseeded gels and a very weak exothermic peak at ~500 °C was detected for all samples, irrespective of the introduction of the seed. It is implied that this peak is related to the formation of pyrochore and/or perovskite phase, and the X-ray diffraction measurement confirms this conclusion.
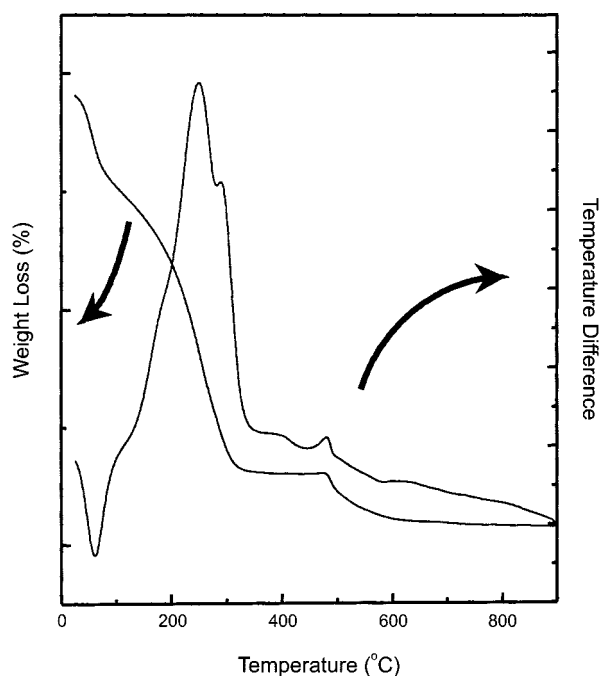

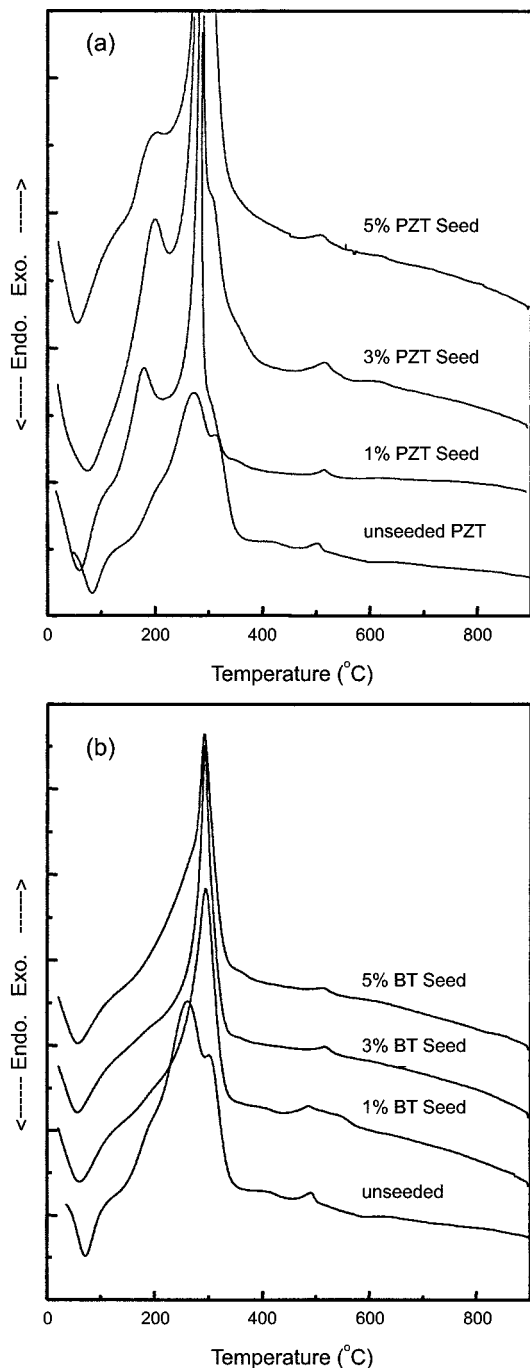**Figure 1**. DTA and TGA curves for the unseeded PZT gel powder.

Figure 2. DTA curves of PZT gel powder seeded with various amounts of 1.2 μm size (a) PZT and (b) BT seed.

The amorphous PZT phase was reported to transform to a metastable pyrochlore at temperature as low as 350 °C, finally to form the perovskite phase at temperatures higher than 500 °C. Mackenzie[17] and Desu[15] studied the kinetics of the pyrochlore to perovskite phase transfomation of sol-gel derived PZT films. The phase transformation kinetics was described as a consecutive reaction process in which nucle-ation dominated. Therefore, the addition of seed particles introduced nucleation sites in the form of low-energy epitaxial interfaces and thereby selectively increased the
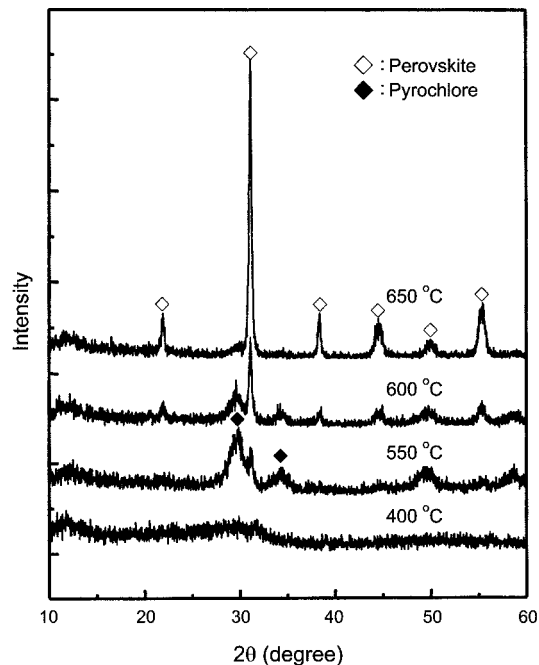

Figure 3. XRD patterns of unseeded PZT powders heated at various temperature for 1 hour.

crystallization rate of the phase that is isostructural with the seed particle.

XRD patterns of unseeded PZT powders as a function of firing temperature are given in Figure 3. It can be seen that peaks corresponding to a pyrochlore phase appeared along with a weak perovskite (110) peak at 550 °C. However, further heating promoted the development of perovskite phase, so that by 650 °C, virtually all of the pyrochlore was transformed to perovskite phase.

The XRD patterns of seeded PZT powders are shown in Figure 4. It is clear from the figure that the perovskite phase started to grow at temperature as low as 400 °C, since the expected perovskite phase can grow from the gel matrix onto the provided nuclei along certain crystallographic directions. For seeded samples, single perovskite phase was obtained at 550 °C, almost 100 °C lower than unseeded case. This lowering in temperature was attributed to the fact that heterogeneous nucleation eliminates the need for the system to exceed the activation energy required for the formation of the nuclei as in the case of a system with homogeneous nucleation. In Figures 5 and 6, percentages of perovskite phase for the seeded PZT samples with different content and size of the seed as a function of temperature are shown.

The relative amounts of perovskite and pyrochlore phases were determined by measuring the relative intensity of XRD peaks by using the following equation[18]:

$$\% \text{ perovskite} = \frac{I_{111}(Pe)}{I_{111}(Pe) + I_{220}(Py)}$$

The amount of perovskite phase formed was promoted with increasing seed content incorporated in the gels, and consequently the formation temperature of pure perovskite
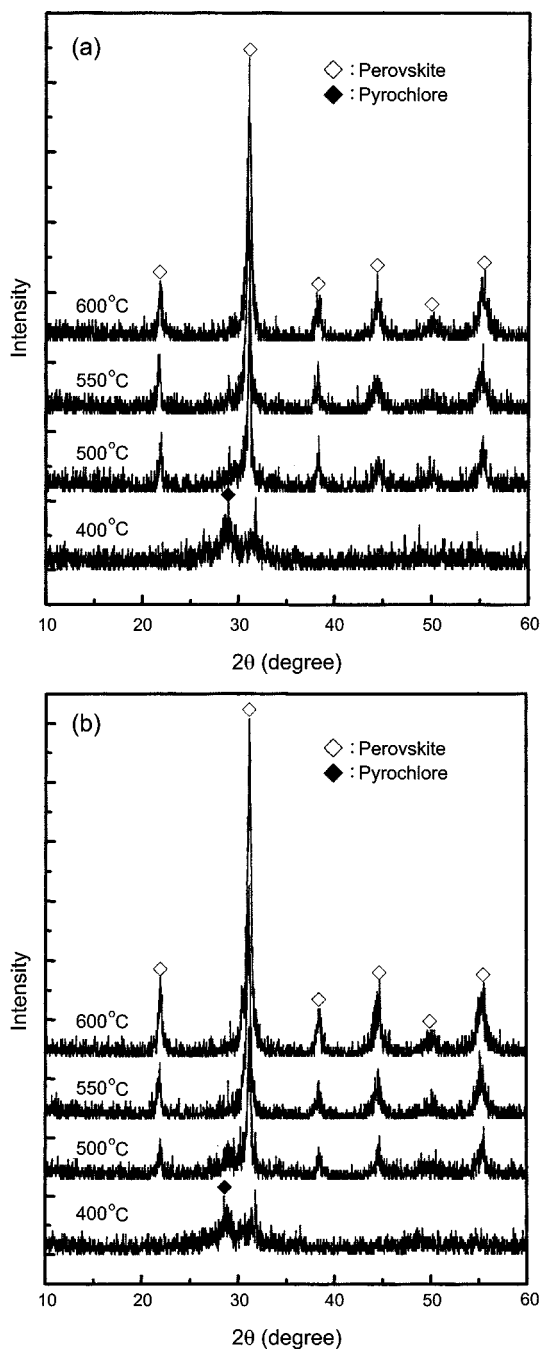
Figure 4. XRD patterns of PZT powders seeded with 3 wt% (a) PZT and (b) BT seed (0.2 μm) heated at various temperature for 1 hour.

Figure 5. Percentage of perovskite phase vs. temperature for the seeded PZT with various concentration of 0.2 μm (a) PZT and (b) BT seed.

phase was lowered as the seed content was increased. As the perovskite nucleation site density increased with the increase of seed concentration, the amount of perovskite phase also increased. The amount of perovskite phase formed in the PZT powder also increased with decreasing seed size when the same weight of seeds are added. It is derived that the decrease of seed size induces increase of surface area and this in turn provides more nucleation sites.

Lead titanate has an ideal cubic perovskite structure above Curie temperature (T_c) with Ti ion at the body center position, 6 O atoms centered on the six cubic faces and Pb
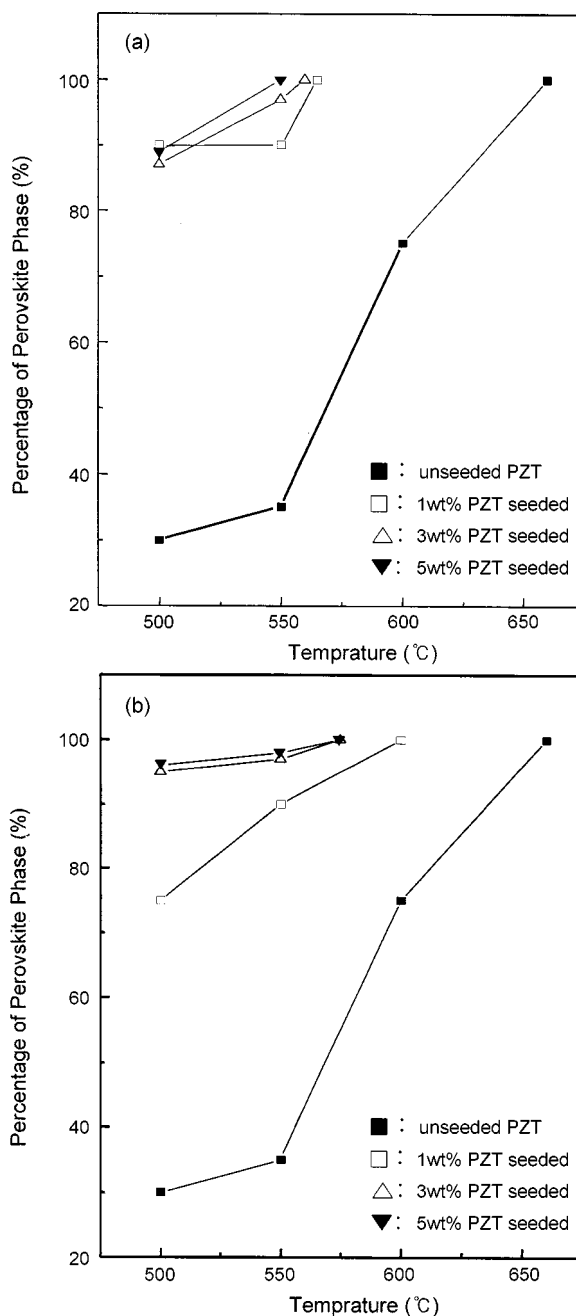
ions at the corners of a cube. The structure can be described as a system of TiO_6 octahedra joined at the corner with Pb ions placed in the interstitial position between the octahedra. In the cubic phase (space group O_h^1), no first order Raman bands are predicted for $PbTiO_3$ crystals. However below T_c, lead titanate is distorted to a tetragonal structure (space group C_{4v}). Triply degenerate T_{1u} mode (IR active only) in cubic phase of O_h^1 splits into two modes transforming as the A_1+E irreducible representations on the tetragonal phase of C_{4v} which are both Raman and IR active.[19] Substitutions of Zr^{+4} for Ti^{+4} on lead titanate in the range x < 0.53 produce a tetragonal phase of the same kind as pure $PbTiO_3$ but with a
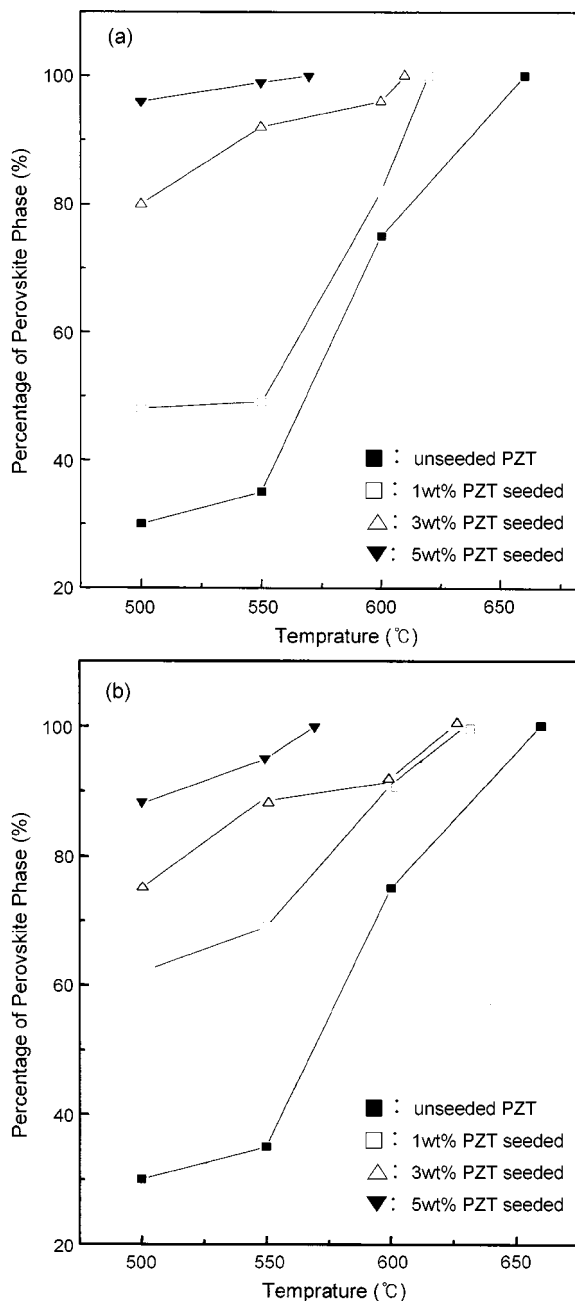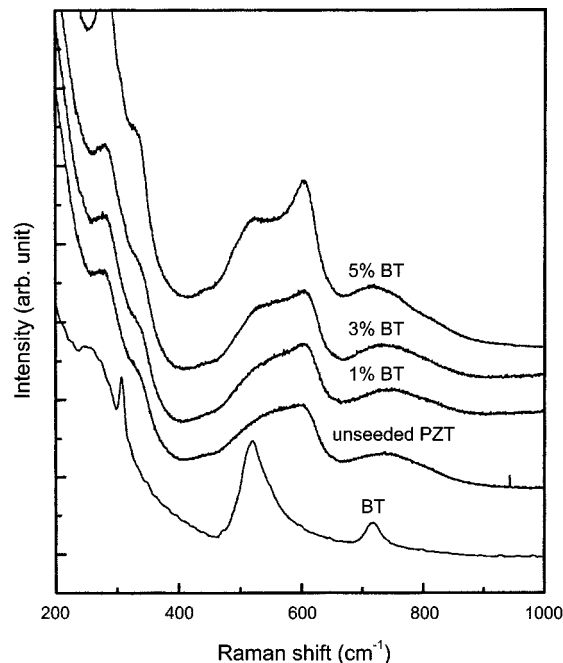
Figure 7. Raman spectra of seeded PZT powders with various concentration of BT seed.

frequency broad peak at ~280 cm^{-1} was attributed to the O-Ti-O bending vibration. It can be seen in the figures that the profile of the very broad peak at ~570 cm^{-1} for unseeded PZT sample remarkably changes to a sharp peak with increasing BT seed concentration. This is an evidence for the increase of crystallinity.

The microstructures of PZT grains grown with BT seed were analyzed by SEM and TEM. The concentration of 0.2 μm-sized BT seeds added to the PZT sol was varied to 1.0-5.0 wt%. As shown in Figure 8, the size of PZT grain increased with the increase of BT seed addition. This is consistent with the results obtained from XRD analysis described in Figures 3 and 4 (b).

The interface between the BT seed and the grown PZT was analyzed with TEM. The BT seed is expected to be imbedded in the core of individual PZT particles. Thus, the particulate PZT samples were sliced by an ultramicrotome with a thickness of 30 nm. Figure 9(a) indicates the cross-section of a PZT particle with imbedded BT seed. The BT seed located in the center of Figure 9(a) was about 0.3 μm in size, and looked more crystallized compared with surrounding medium. The clear diffraction spots indicate that BT seed is highly crystallized and oriented to (111) phase, while the circular patterns indicate the presence of less-crystallized PZT phase. Figure 9(b) shows a high resolution TEM image for the interfacial grain boundary between BT seed and grown PZT. The uniform fringes are observed in the region on the left side, and the gap between these fringes is estimated to be 0.46 nm, which confirms the presence of BT. The uniform fringes formed over the entire BT region indicate that BT seed is a highly crystallized single grain. On the right side of BT region, less-crystallized PZT grains were observed. At the very surface of BT seed PZT layer
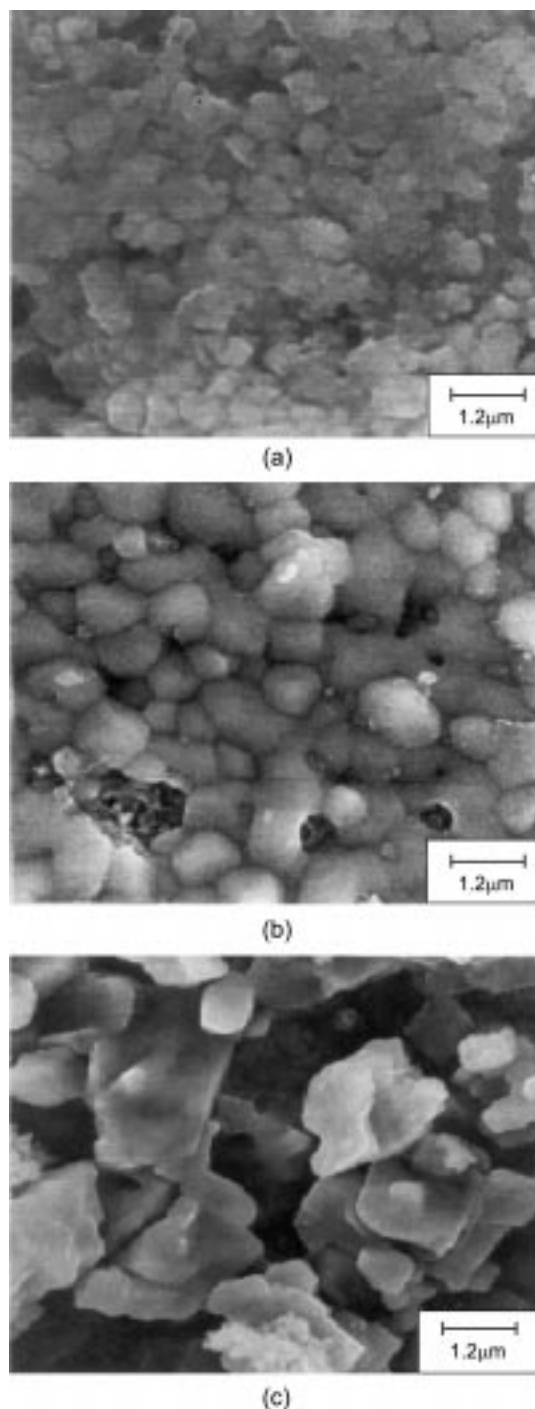
Figure 6. Percentage of perovskite phase vs. temperature for the seeded PZT with various concentration of 1.2 μm (a) PZT and (b) BT seed.

smaller tetragonal distortion.

Figure 7 shows the Raman spectra obtained at room temperature for seeded PZT powders with different BT seed contents between 0 and 5 wt%. The lowest curve in the Raman spectra corresponds to the pure BT powder.

The relatively strong peak at 520 cm^{-1} for BT and a very broad strong peak at about 570 cm^{-1} for unseeded PZT sample can be assigned to the transverse optic mode of the Ti-O stretching vibrations in the TiO$_6$ octahedra with its longitudinal optic pair giving rise to the weak peak at ~710 cm^{-1} (BT) and ~720 cm^{-1} (PZT), respectively.[20-22] The lower

(a)

(b)

(c)

Figure 8. Microstructure of seeded PZT powder with various amounts of BT calcined at 600 °C for 4 hours. (a) 1 wt%, (b) 3 wt%, (c) 5 wt%.

seemed to be grown epitaxially, but soon lots of small polycrystalline PZT grains around 5 nm in size appeared, as shown in the right side of Figure 9(b). This indicates that the growth of PZT is not achieved solely by the heterogeneous nucleation on the surface of BT seed, even though BT seed plays a key role in the formation of perovskite PZT phase. We believe that both the heterogeneous and homogeneous nucleation contributes competitively in the formation of perovskite PZT.
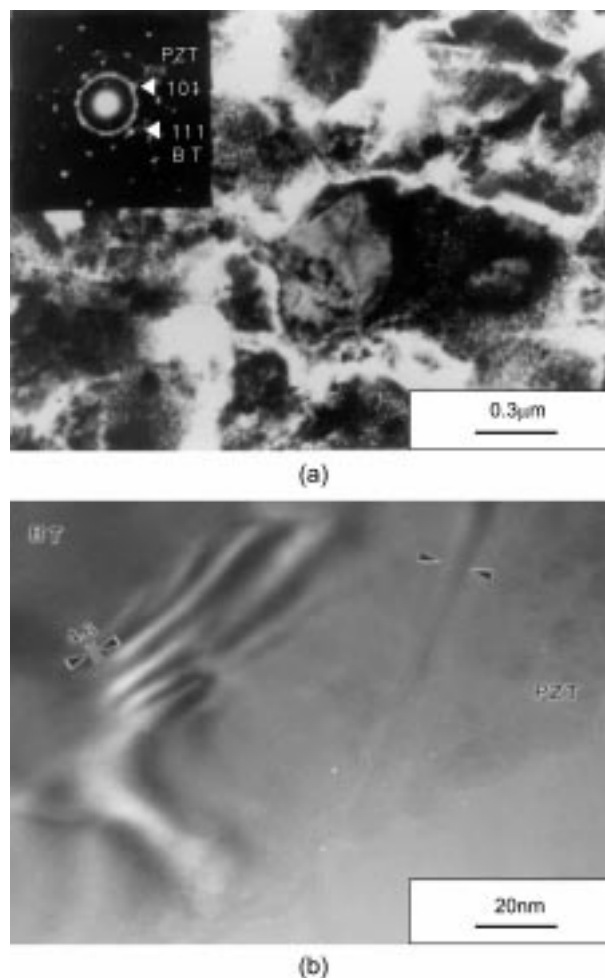

(a)

(b)

Figure 9. TEM image and diffraction pattern of BT seeded PZT powders. (a) low magnification image with diffraction pattern; (b) high magnification image of the interface between BT seed and PZT.

Conclusions

By introducing BT or PZT seeds in the PZT sol-gel system, polycrystalline PZT powders in pure perovskite phase could be obtained at 550 °C, which was about 100 °C lower than the unseeded case. The seeding effect of BT and PZT seed was not appreciably different. This is attributable to their similarities in crystallographic structure and lattice parameters. The seeding effect was proportional to the concentration of introduced seed, and the seeds with smaller size gave greater effect. This suggests that the nucleation of PZT grains started mainly on the surface of BT or PZT seeds. However, the high resolution TEM images for the interface between the BT seed and PZT indicate that both the heterogeneous and homogeneous nucleation contribute competitively in the formation of perovskite PZT.

References

1. Jaffe, B.; Roth, R. S.; Marzullo, S. *J. Appl. Phys.* **1954**, *25*, 809.
2. Moazzami, R.; Hu, C.; Shepherd, W. H. *IEEE Trans. Electron Device* **1992**, *39*, 2044.
3. Buchanan, R. C. *Ceramic Materials for Electronics*, 2nd ed.; Marcel Dekker: New York., 1991; p 186.
4. Liu, D.; Zhang, H.; Wang, Z.; Zhao, L. *J. Mater. Res.* **2000**, *15*, 1336.
5. Wu, A.; Vilarinho, P. M.; Salvado, I. M. M.; Baptista, J. *J. Am. Ceram. Soc.* **2000**, *83*, 1379.
6. Kim, A.; Jun, M.; Hwang, S. *J. Am. Ceram. Soc.* **1999**, *82*, 289.
7. Zhang, Q.; Whatmore, R.; Vickers, M. E. *J. Sol-Gel Sci. and Tech.* **1999**, *15*, 13.
8. Bagwell, R. B.; Messing, G. L. *J. Am. Ceram. Soc.* **1999**, *82*, 825.
9. Liu, C.; Komarneni, S.; Roy, R. *J. Am. Ceram. Soc.* **1992**, *75*, 2665.
10. Chen, M.; James, P. F.; Lee, W. E. *J. Sol-Gel Sci. and Tech.* **1994**, *1*, 99.
11. Okuyama, M.; Fukui, T.; Sakurai, C. L. *J. Mater. Res.* **1992**, *7*, 2281.
12. Ravindrauathan, P.; Komarneni, S.; Roy, R. *J. Am. Ceram. Soc.* **1990**, *73*, 1024.
13. Carvalho, J. C.; Paiva-Santos, C. O.; Zaghete, M. A.; Oliveira, C. F.; Varela, J. A.; Longo, E. *J. Mater. Res.* **1996**, *11*, 1795.
14. Chen, Y. F.; Nass, R. *J. Sol-Gel Sci. and Tech.* **1997**, *8*, 385.
15. Kwok, C. K.; Desu, S. B. *J. Mater. Res.* **1994**, *9*, 1728.
16. Othman, B. M.; Suzuki, H.; Murakami, K.; Kaneko, S.; Hayashi, T. *IEEE Trans. Electron Device* **1996**, *2*, 731.
17. Chen, K. C.; Mackenzie, J. D. *Mat. Res. Soc. Sym. Proc.* **1990**, *180*, 663.
18. Lakeman, C. D. E.; Payne, D. A. *J. Am. Ceram. Soc.* **1992**, *75*, 3091.
19. Zhang, H.; Uusimaki, A.; Leppavuori, S.; Karjalainen, P. *J. Appl. Phys.* **1994**, *76*, 4294.
20. Lurio, A.; Burns, G. *J. Appl. Phys.* **1974**, *45*, 1986.
21. Taguchi, I.; Pignolet, A.; Wang, L.; Proctor, M.; Lévy, F.; Schmid, P. E. *J. Appl. Phys.* **1993**, *74*, 6625.
22. Last, J. T. *Phys. Rev.* **1957**, *105*, 1740.